RESEARCH ARTICLE

BULLETIN OF SCIENTIFIC RESEARCH

Asian Research Association

DOI: 10.54392/bsr2421

Modelling and Simulation of Refractive Index-Based FBG Sensor for the Detection of Blood, Adrenal, Cervical, Breast and Skin Cancers

L. Vincent Raj [1,*], N. Srinivasan [1], Preeta Sharan [2], Anup M Upadhyaya [3]

[1] Department of Physics, Thiagarajar College, Madurai, Tamil Nadu, India
[2] Department of Electronics and Communication Engineering, The Oxford College of Engineering, Bangalore, India
[3] Department of Mechanical Engineering, The Oxford College of Engineering, Bangalore, India
*Corresponding author Email: josephvincent2002lp@gmail.com
DOI: https://doi.org/10.54392/bsr2421
Received: 22-06-2024; Revised: 09-10-2024; Revised: 18-10-2024; Published: 03-11-2024

Abstract: Cancer cell detection is critical to early diagnosis and treatment, aiming to improve patient outcomes through timely interventions. One promising approach involves using Fiber Bragg Grating (FBG) sensors due to their high sensitivity, biocompatibility, and ability to operate in real time. Due to the blood's refractive index, the wavelength shift in an FBG sensor varies, leading to a change in the effective refractive index. This occurs because the interaction between the FBG sensor and the surrounding medium, like blood, alters the light propagation within the fiber. The shift in the reflected wavelength corresponds to changes in the effective refractive index, which can be used to detect cancer- related anomalies in the blood. However, the proposed grating structure provides a wavelength shift between 1.43184 and 1.47500 with an effective refractive Index between 1.360015 and 1.401017. Besides all wavelength shifts and effective refractive Index have been proposed for Blood, cervical, Adrenal, Breast, and Skin cancers. The wavelength vs effective refractive index relationship for various cancerous cells has been established.

Keywords: FBG, Fibre Optics, Refractive Index, Resonant Wavelength Shift, Cancerous Cell

1. Introduction

Improving the quality of an individual's life for healthcare management is directly related to the patient's engagement in health prevention. The ability to diagnose and cure illnesses is becoming more advanced because of recent scientific and technological advancements. The main technologies that are facilitating this digitization of health care which is leading to customized care and innovative healthcare systems. One significant area of concern is cancer, which is defined by unchecked cell proliferation or uncontrolled cell division. It impacts every part of the human system, mainly the blood or lymphatic. Mammography, ultrasound, MRI, biopsy, and complicated blood tests are only a few of the several early cancer detection procedures that are either difficult, expensive, uncomfortable, or have low sensitivity and accuracy. It's not just for cancer diagnosis; it's also for several blood-related illnesses like HIV, malaria, and other infections. Thus, to identify all of these types of impacted cells at an early stage, there should be a need for straightforward, non-invasive, and primarily inexpensive detection techniques that can detect diseases at an early stage, improving patient outcomes and reducing the burden on healthcare systems [1].

One of the promising innovations in this regard is Fiber Bragg Gratings (FBGs), initially developed in the 1990s for telecommunications. These optical devices have since been adapted for use in sensing technologies, revolutionizing various fields, including healthcare. The basis for the sensing principle of FBG used in sensing is predicated on identifying the Bragg wavelength shift. Brought about by variations in the effective refractive index or grating period. Fiber Braggs gratings are spectral filters that are made inside the segments of optical fibers [2]. In general, FBG transmits all wavelength ranges while reflecting light within a small range but it is possible to modify them to have more complex spectral responses. The FBG is produced by periodically modulating the refractive index along the fiber's core. The constant or uniform grating, in which the refractive index modulation has a constant period along the grating segment, is the most basic structural component of FBGs. These fundamental FBGs provide a reflected spectrum with a peak centered at the Bragg's wavelength. FBGs have the advantage of operating in both transmission and reflection modes [3]. Most likely, It is possible for the Fiber Braggs grating to be engaged as a thermal sensor with high sensitivity and accuracy to measure temperature difference because tumors have higher blood flow and metabolic

rates than normal tissues, there are temperature disparities between the two types of tissues. As a result, temperature is an important indicator of cancer diagnosis. One particularly valuable application in the medical field is thermal sensing for cancer diagnosis, where temperature differences between cancerous and normal tissues—due to tumors' increased blood flow and metabolic rates— is highly sensitive and accurate to measure [4]. In biosensing, shifts in the Bragg wavelength caused by changes in the refractive index of biological samples allow FBGs to function as highly sensitive bio-detectors. This sensitivity positions FBGs as a promising tool for early cancer detection, as they can detect even the smallest variations in the refractive index that are linked to the presence of cancerous cells [1]. Biosensors are one of the key technologies enabling this digital revolution in healthcare since they generate high sensitivity and are effective in tracking customized treatments and patient-specific care. In the market today, electrically based sensors continue to rule. However, they require regular calibration and are subject to electromagnetic interference. To overcome the disadvantage, scientists introduce optic sensing and its various applications. Here, light is the primary carrier of the signal rather than electron movement. Unlike other forms of sensors, fiber optic sensors are free from electromagnetic interference and provide responses at a faster rate [3].

In this paper, we fully focused on the Fiber Braggs grating sensor for the detection of cancer cells. Here, the FBG-related optical biosensor is introduced. The process of fabricating FBGs is technically demanding and somewhat complicated process that calls for sophisticated technologies like femtosecond layers and laser interference systems. Key fabrication techniques include the laser interference method, the point-by-point approach, and the phase mask method, each contributing to the precise creation of the grating structure within the optical fiber [3]. Simplification in design with optimized accuracy and sensitivity provides easier fabrication with better results for the detection of cancerous cells: blood cancer, cervical cancer, gland cancer, breast cancer of type-I and type-II, and skin cancer. Here, we can determine how much wavelength is shifted by using the various refractive indices for various cancerous cells to provide an effective refractive index for each cancerous cell, which can then be analyzed. In this paper, we fully focused on the Fibre Braggs grating sensor for the detection of cancer cells [5].

2. Types of Cancer

2.1 Blood Cancer

Cancers that affect the blood, bone marrow, or lymphatic system are referred to as blood cancers or hematologic cancers. Three main types of blood cancer are leukemia, lymphoma, and myeloma, which refer to cancers of the bone marrow's plasma cells, lymphatic system, and blood, respectively. The causes and risk effects are genetic mutation, exposure to radiation or chemicals, family history, viral infections (e.g., HIV, HT LV-1), and immunodeficiency disorders. The most common symptoms are fatigue, weight loss, swollen lymph nodes, shortness of breath, etc. The diagnosis of this cancer should be lymph node biopsy, imaging tests, bone marrow biopsy, and blood chemistry. The treatment of this blood cancer is most likely chemotherapy, radiation therapy, and Immunotherapy [1].

2.2 Cervical Cancer

Cervical cancer is a kind of uterine cancer that may occur in women. The cervix is located at the base of the uterus. Human papillomavirus (HPV) infection, unprotected sexual activity, compromised immune system, smoking, and other risk factors are among the causes. Pelvic pain or discomfort, irregular vaginal bleeding, and other similar symptoms are frequent with cervical cancer. The diagnosis for this cancer is a Pap test, HPV test, colposcopy, and biopsy. The treatment taken for this cancer is hysterectomy, radiation therapy, chemotherapy, and targeted therapy [1, 2].

2.3 Adrenal Cancer

Adrenal cancer, sometimes referred to as adrenocortical carcinoma (ACC), is a rare or uncommon and aggressive kind of cancer that develops in the adrenal glands. Causes and Risk Factors are Genetic mutations (Li-Fraumeni syndrome, Beckwith-Wiedemann syndrome) Family history, radiation exposure, and Hormonal imbalances. The Symptoms related to this cancer are Weight gain (particularly in the midsection), Weakness or fatigue, High blood pressure, Diabetes, Deepening voice, Excessive hair growth (hirsutism), Abdominal pain or discomfort, Nausea, and vomiting. The diagnosis can be imaging tests like CT, MRI, & PET, and then a biopsy. The treatment given for Adrenal cancer is adrenalectomy, chemotherapy, hormone therapy, and so on [1, 5].

2.4 Breast Cancer

Cancer that develops in the breast tissue is known as breast cancer. Women over 50 are typically affected by breast cancer, however, women and people with AFAB under 50 can also be affected. Furthermore, breasts could affect males and those with an Assigned Male at Birth (AMAB). Researchers often use the MDA-MB-231 human breast cancer cell line. Prefix "MDA" stands for "Molecular Diagnosis and Therapy," which means that the cell line originated from the MD Anderson Cancer Centre at the University of Texas. If

a cell line ends in "MB: Metastatic Breast," it means the tumour from whence it originated spread throughout the body. 231: This identifies the particular cell line. We now know a lot more about the biology of breast cancer thanks to this cell line, and we have new ways to treat the disease. A different kind of breast cancer cell is the often used human breast cancer cell line, MCF-7 [4, 5]. The most frequent signs of breast cancer are changes in size or form, lumps or thickening, dimpling or puckering, redness or scaliness, pain or discomfort, and so on. Radiation therapy, chemotherapy, targeted therapy, or surgery (lumpectomy, mastectomy) should be used to treat breast cancer [6].

2.5 Skin Cancer

Skin cancer is the most common type of cancer worldwide. Skin cancer is the development of abnormal cells in the skin's tissues. Melanoma, squamous cell carcinoma (SCC), and basal cell carcinoma (BCC) are the three most prevalentforms of skin cancer. Skin cancer is mostly diagnosed by abnormal growths or lesions that fluctuate in size, form, or color. Itching or discomfort, bleeding or seeping, and ulcers or scarring. Skin malignancies can be treated with radiation therapy, chemotherapy, immunotherapy, surgery, and Targeted therap [1, 5].

3. Properties and Principles of FBG Sensing

A fiber Bragg grating is a periodic or aperiodic alteration in the effective refractive index within the core of the optical fiber [3]. The duration often spans hundreds of nanometres or beyond that of long- period fiber gratings. The perturbation is approximately periodic across a defined length, such as many millimeters or centimeters. Perturbation has a quasi-periodic nature over a defined length, often ranging from a few millimetres to centimeters.

Because of its easy manufacturing measures and reasonably high reflected signal, fiber Bragg grating (FBG) is the most widely used optical fiber sensor for temperature or strain measurements [6]. It is necessary to review Bragg Law before delving into the theory of Fiber Bragg Grating.

Sir William Lawrence Bragg made the discovery of the Bragg Law of X-ray Diffraction in 1912. Even now, the theory is applied to the investigation and determination of crystal structure. A wave interacting with a crystalline substance and scattering and diffracting causes Braggs diffraction.

The Braggs law equation explains this phenomenon. The Braggs law equation is $n\lambda = 2\,d \sin\theta$ where n, λ, θ, and dare integers, wavelength, incident angle, and distance between the atomic layers respectively [6]. This formula elucidates why, at certain angles of incidence, the surfaces of crystals reflect X-ray radiation. Comparable to an optical fiber grating, a diffraction structure is defined by periodic changes to the refractive index at the fiber's core.

In order to achieve a controlled and efficient power transfer between optical fiber modes, this structure satisfies the phase-matching condition between the co-propagating fundamental core mode and other modes, such as cladding modes, radiation (or leaky) modes, additional modes, or counter propagating core modes [7]. The grating pitch L, which is the period of refractive index modulation, allows OFGs to be classified as either short-period gratings, or fibre Bragg gratings (FBGs), or long-period gratings (LPGs).

The grating pitch of a fibre Bragg grating (FBG) is typically hundreds of nanometres in size. Because of the grating area's ability to reflect and transmit part of an optical signal, this arrangement makes it easier to phase-match the basic core mode with its corresponding counter propagating core mode.

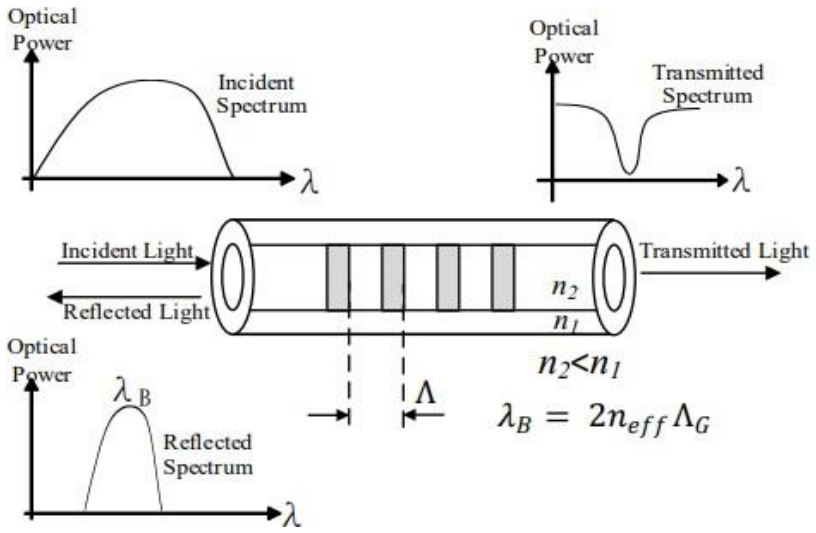

Figure 1. Schematic of the long-period grating fiber [3]

The Braggs phase matching condition [1] is, $\boldsymbol{\lambda B = 2neff\Lambda}$. here, λB, $neff$ and Λ are brags wavelength or resonant wavelength, effective refractive Index, and Grating Pitch. When operating essential patterns, the FBG, which is engraved in standard single-mode fiber, is naturally sensitive to atmospheric RI. The FBG is a common temperature sensor [1, 8].

$$\frac{dyB}{dT} = \lambda_B \frac{1}{\Lambda}\frac{d\Lambda}{dT} + \lambda_B \frac{1}{neff}\frac{dn_{eff}}{dT} \quad (1)$$

$$\frac{dyB}{dT} = (a+\zeta) \times \lambda_B (X+a)^n \quad (2)$$

$$a = \frac{1}{\Lambda}\frac{d\Lambda}{dT} \quad (3)$$

$$\zeta = \frac{1}{\Lambda}\frac{d\Lambda}{dT} \quad (4)$$

For the optical fiber material, $\boldsymbol{\zeta}$ is a thermal Optical Coefficient and a is a thermal expansion coefficient. Impacts from thermo-optics and thermal expansion on the effective refractive index of the grating period and modes as a function of temperature change are mostly caused by variations in the material scale and grating period. Here is a representation of the FBG temperature sensitivity coefficient:

$$K_r = \frac{1}{\lambda_B}\frac{d\lambda B}{dT} = a + \zeta \quad (5)$$

Finally, the wavelength change and temperature are related,

$$\frac{dy_B}{\lambda_B} = (a+\zeta) \times VT \quad (6)$$

A change in pressure causes the Bragg wavelength shift ΔP is explained by, [9, 10]

$$\Delta\boldsymbol{\lambda_P} = \lambda_B \left[-\frac{(1-2v)}{E} + \frac{n_{eff}^2}{2E}(1-2\vartheta)(2P_{12}P_{11})\Delta P \right. \quad (7)$$

4. Model of FBG

4.1 Coupled Mode Theory (CMT)

One of the greatest instruments for studying the optical characteristics of gratings, the CMT will be investigated for use in modeling the FBG. When studying optical waveguides and how waves interact with materials, the CMT is an effective mathematical tool. The grating structure is seen by the CMT as an optical waveguide disruption. [11] The findings demonstrate an outstanding agreement with experimental investigations, and CMT has been effectively used to simulate a variety of fiber grating systems. The fabrication of FBG results in a perturbation on the effective refractive index neff of the guided modes which is given by [12].

$$\delta_{neff}(Z) = \delta_{neff}^{-}(Z)\left\{1 + v\cos\left[\frac{2\pi_Z}{\Lambda} + \phi(Z)\right]\right\} \quad (8)$$

δ_{neff} indicates 'dc' index change, v gives the fringe visibility of the index change, $\boldsymbol{\Lambda}$ is the grating period and $\boldsymbol{\phi(z)}$ is the grating chirp.

The simplified coupled mode equations for a single-mode FBG are provided as [12].

$$\frac{dR}{dZ} == \mathrm{i}\hat{\sigma}\mathrm{R(z)} + \mathrm{ikS(z)} \quad (9)$$

$$\frac{ds}{dz} = i\hat{\sigma}R(z) - ik^*R(z) \quad (10)$$

Where R(z) and S(z) are the amplitudes of forward propagating and backward propagating modes respectively. K is the "ac" coupling coefficient.$\hat{\sigma}$ is the general "dc" coupling coefficient. They are defined as,

$$\hat{\sigma} = \delta + \sigma - \frac{1}{2}\frac{d\emptyset}{dZ} \quad (11)$$

$$K - K^* = \frac{\pi}{\lambda} v\delta_{neff}^{-} \quad (12)$$

The detuning δ and σ in eqn 11 are defined as,

$$\delta = \beta - \frac{\pi}{\Lambda} = 2\pi n\left(\frac{1}{\lambda} - \frac{1}{\lambda_D}\right) \quad (13)$$

$$\sigma = \frac{2\pi}{\lambda}\delta_{neff}^{-} \quad (14)$$

With a uniform FBG, the grating chirp $d\phi/dZ$ =0, equations (11), (12), and (14) are constants, and $\beta neff$ is the mode propagation constant. Through the specification of suitable boundary conditions, the reflectivity's analytic expression can be found as follows [12, 13]

$$r = \frac{sin^2(\sqrt{k^2-\hat{\sigma}L}}{Cos^2\left(\sqrt{k^2}-\sigma L\right)-\frac{\partial^2}{k^2}} \quad (15)$$

5. Results and Discussion

Figure 2, 3, 4 & 5 Indicate the Fiber Braggs Grating Material Display Profile.

The parameters of the FBG utilized for the simulation are specified in Table 1. The simulation was run using Rsoft Grating MOD, and the spectrum response of a Fiber Braggs Grating is obtained.

5.1 Blood Cancer

Figure 6 shows the variation of relative power vs wavelength of blood cancer obtained using the Rsoft software.

5.2 Cervical Cancer

Figure 7 shows the variation of relative power vs wavelength of cervical cancer obtained using the Rsoft software.

5.3 Adrenal Cancer

Figure 8 shows the variation of relative power vs wavelength of blood cancer obtained using the Rsoft software.

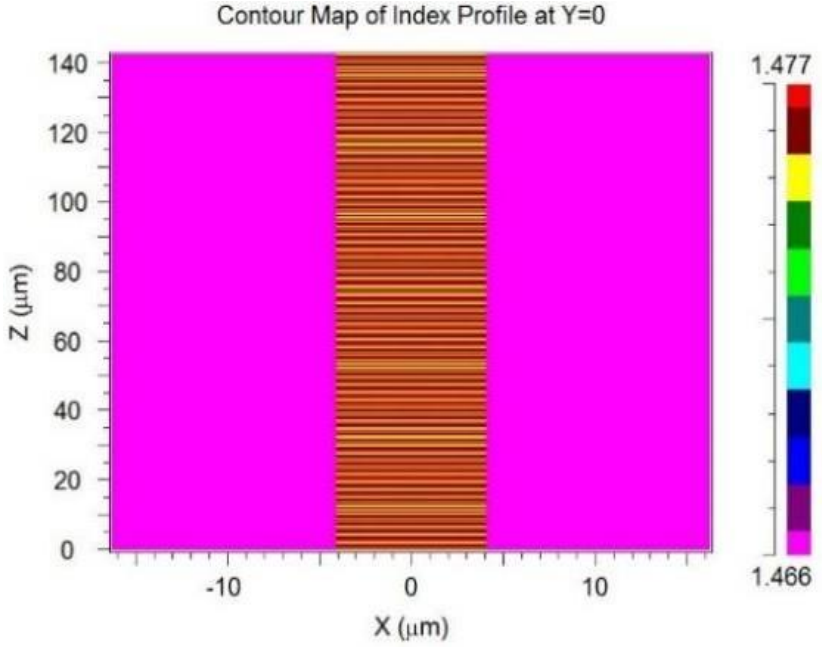

Figure 2. Material Profile Contour Map Xz

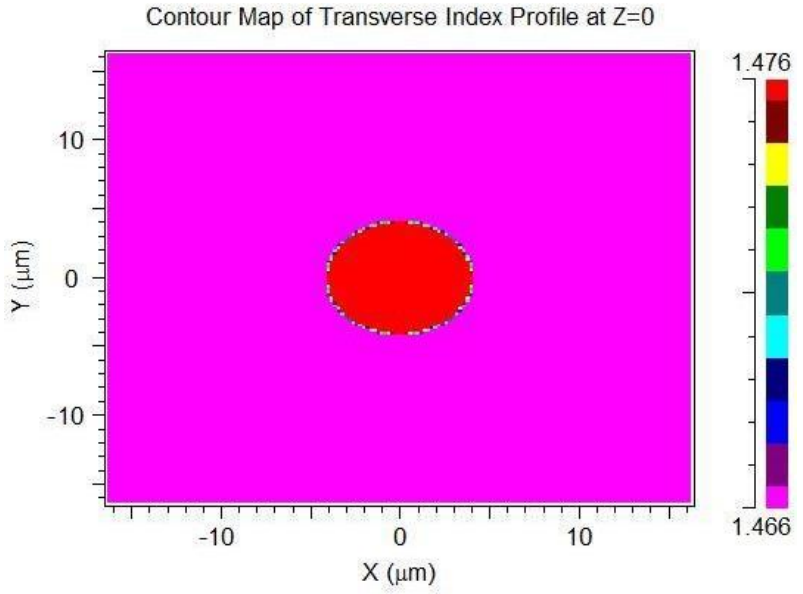

Figure 3. Material Profile Contour Map Xy

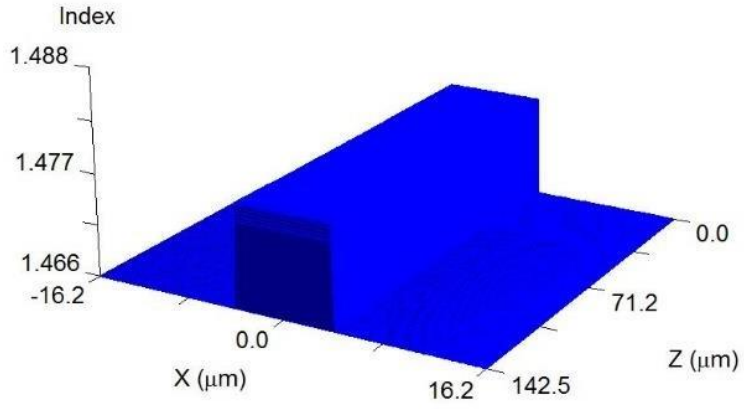

Figure 4. Material Profile 3d Slices

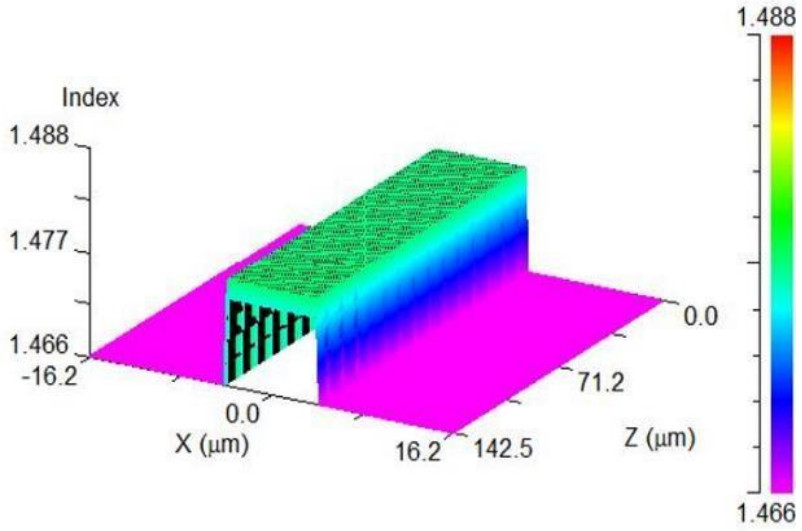

Figure 5. Material Profile Height Coded

Table 1. Simulation Parameters of FBG Using Rsoft Grating Mod

Simulation Tool	**Grating MOD**
Type of Profile	Step Index, single mode
Type of Structure	Fiber
Type of Grating	Volume Index
Component Height	8.2
Component Width	8.2
Index Difference	Delta*1.1
Delta	0.001
Period	0.5264
Free space Wavelength	1.55[um]

Table 2. Different Types of Cancer Cells with Normal and Affected Cell Ri

Types of Cancer	**Cancer Cell Type**	**Ri of Cancer Affected Cell**	**Ri of Normal Cell**	**References**
Blood Cancer	Jurkat	1.390	1.376	[14], [15],[16]
Cervical Cancer	Hela	1.392	1.368	[14], [15],[16]
Adrenal Cancer	PC-12	1.395	1.381	[14], [15],[16]
Breast Cancer	(MDA)-(MB)-231	1.399	1.385	[14], [15],[16]
Breast Cancer	MCF-7	1.401	1.387	[14], [15],[16]
Skin Cancer	Basal	1.380	1.360	[14], [15],[16]

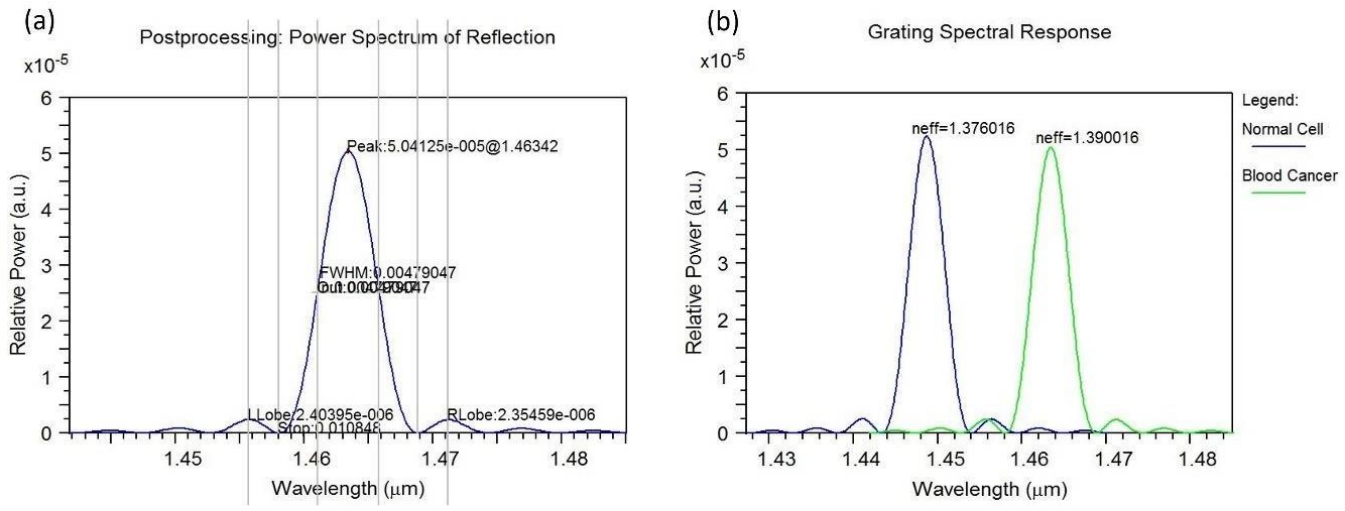

Figure 6 (a) Simulation of a graph that indicates wavelength vs relative power of the blood cancer cell, **(b)** Comparative analysis demonstrates how the reflected wavelengths of cancer-affected and normal cells differ.

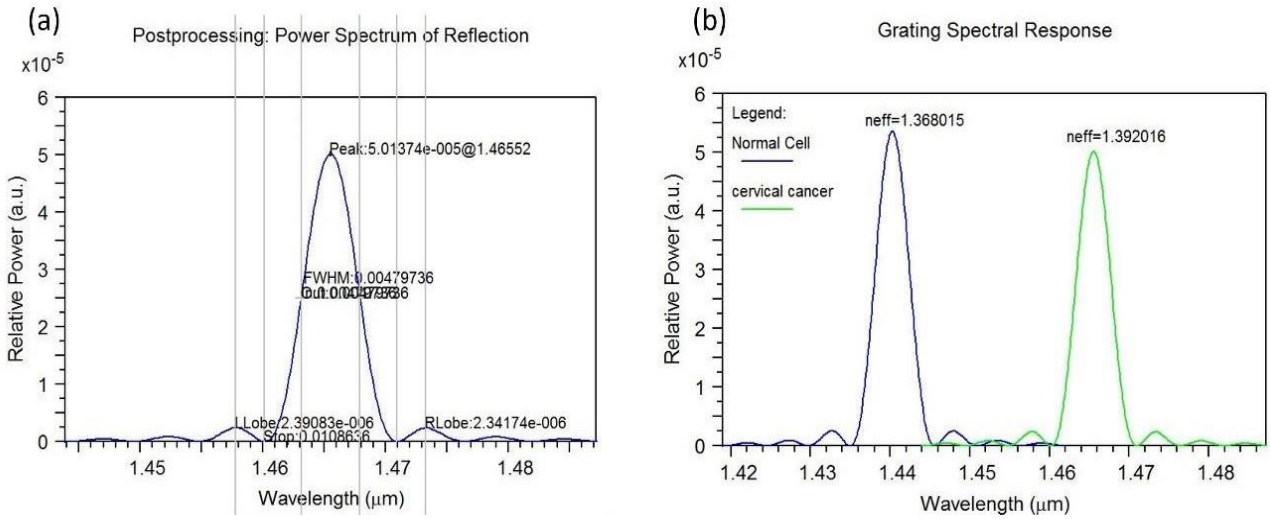

Figure 7 (a) Simulation of a graph that indicates wavelength vs relative power of the cervical cancer cell, **(b)** Comparative analysis demonstrates how the reflected wavelengths of cervical-affected and normal cells differ.

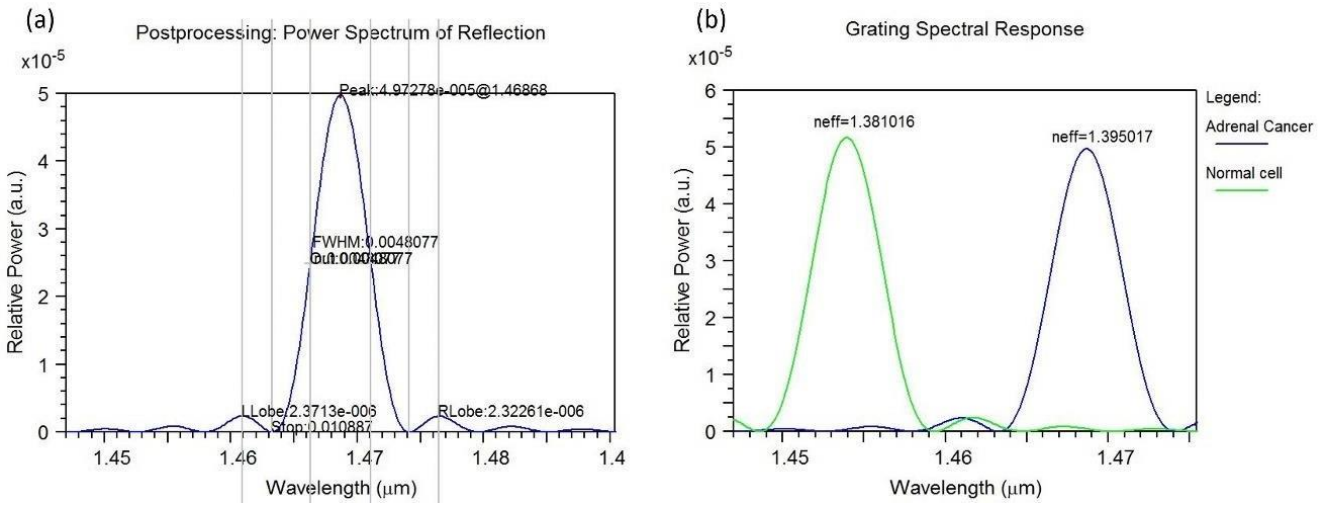

Figure 8 (a) Simulation of a graph that indicates wavelength vs relative power of the Adrenal cancer cell **(b)** Comparative analysis demonstrates how the reflected wavelengths of Adrenal-affected and normal cells differ.

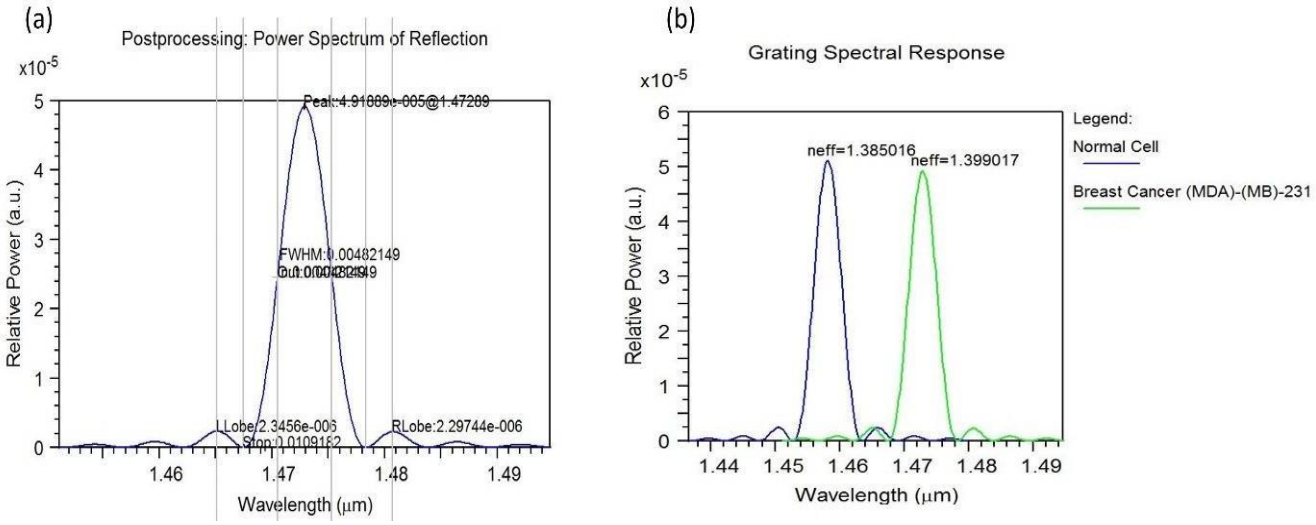

Figure 9 (a) Simulation of a graph that indicates wavelength vs relative power of the breast cancer (MDA)-(MB)-231cell **(b)**Comparative analysis demonstrates how the reflected wavelengths of Breast cancer (MDA)-(MB)-231-affected and normal cells differ.

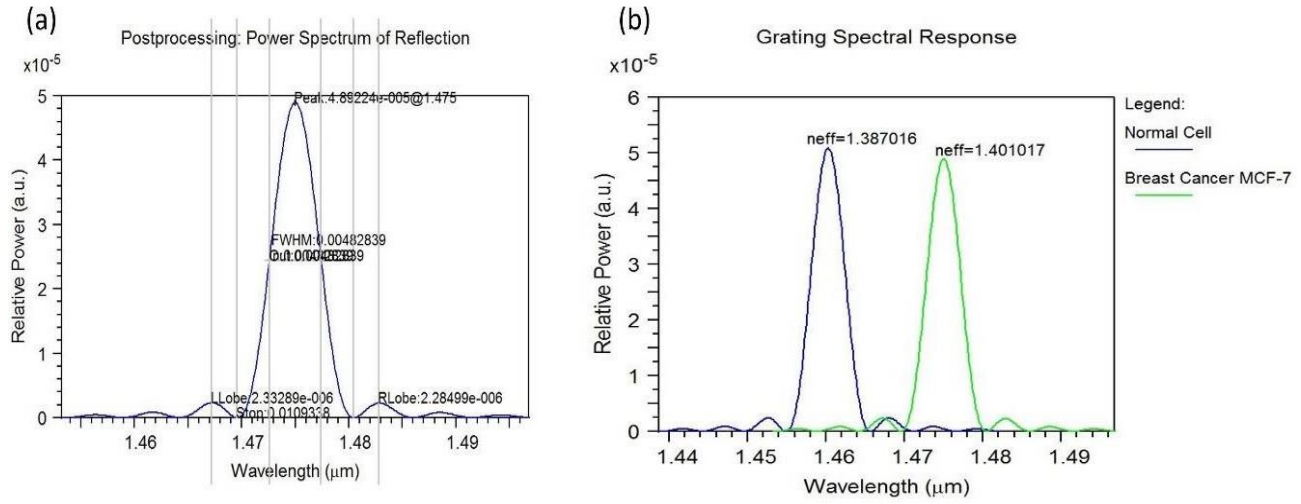

Figure 10 (a) Simulation of a graph that indicates wavelength vs relative power of the breast cancer (MDA)-(MB)-231cell **(b)**Comparative analysis demonstrates how the reflected wavelengths of Breast cancer (MDA)-(MB)-231-affected and normal cells differ.

5.4 Breast Cancer- (Mda)-(Mb)-231

Figure 9 shows the variation of relative power vs wavelength of blood cancer obtained using the Rsoft software.

5.5 Breast Cancer Mcf-7

Figure 10 shows the variation of relative power vs wavelength of blood cancer obtained using the Rsoft software.

5.6 Skin Cancer

Figure 11 shows the variation of relative power vs wavelength of blood cancer obtained using the Rsoft software.

The Table 2 shows Different Types of Cancer Cells with Normal and Affected Cell Ri. The table 3 shows the effective refractive Index for all the cancers and it also reveals the respective wavelength shift for a particular cancer cell.

The Bragg wavelength is the particular light wavelength that is reflected by a FBG sensor. The fiber core's refractive index and the grating time determine the Bragg wavelength. [17] A shift in the Bragg wavelength can result from any modification to the refractive index of the surrounding medium. [18] Bioreceptors that particularly bind to cancer biomarkers can be used to functionalize FBG sensors for cancer cell detection. [4] These biomarkers (cancer cells), alter the optical characteristics of the FBG, particularly the surrounding refractive index when they attach to the bio-receptors.

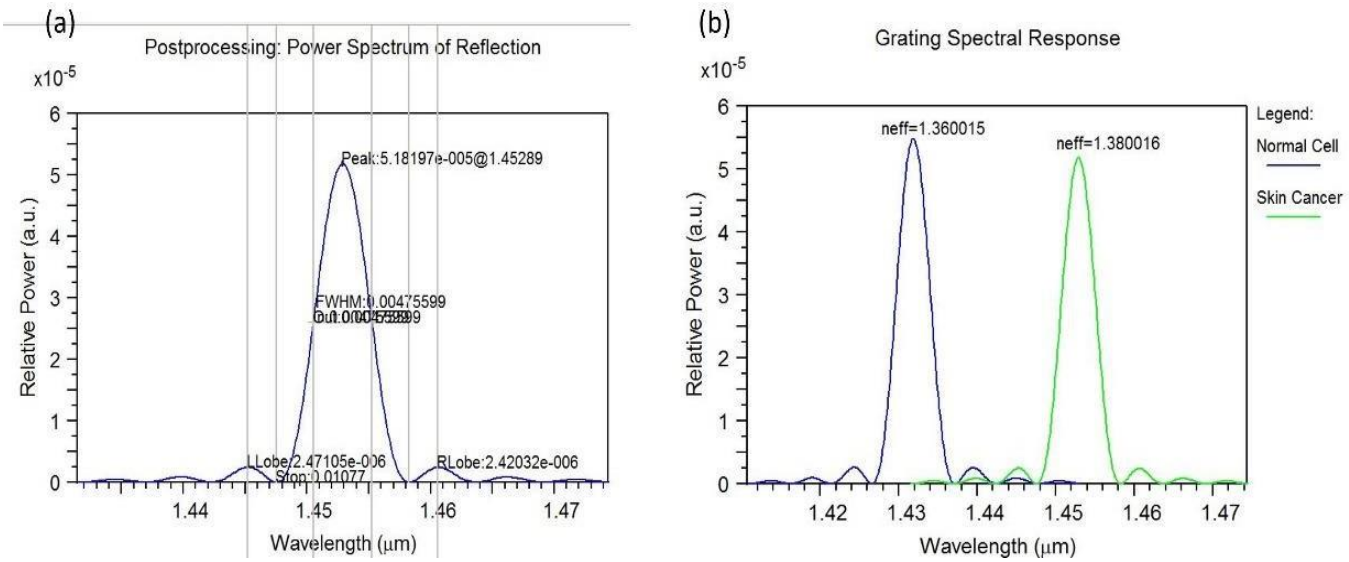

Figure 11. (a) Simulation of a graph that indicates wavelength vs relative power of the skin cancer cell **(b)** Comparative analysis demonstrates how the reflected wavelengths of Skin cancer affected and normal cells differ.

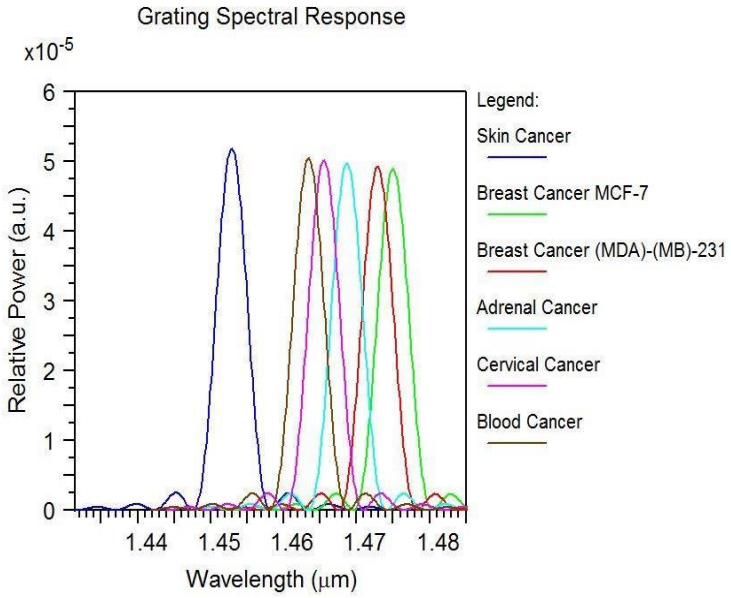

Figure 12. Effect of Wavelength on Relative Power of FBG for Different Cancerous Cell

Table 3. Shows The Result Summary. The Result Shows The Effective Refractive Index Obtained for all types of cancers

Cells		Refractiv E Index	Resonant Wavelength Shift [Um]	Effective Refractive Index (Neff)
Jurkat	Normal	1.376	1.44868	1.376016
	Affected	1.390	1.46342	1.390016
HeLa	Normal	1.368	1.44026	1.368015
	Affected	1.392	1.46552	1.392016
PC-12	Normal	1.381	1.45394	1.381016
	Affected	1.395	1.46868	1.395017

(MDA)-(MB)-231	Normal	1.385	1.45816	1.385016
	Affected	1.399	1.47289	1.399017
MCF-7	Normal	1.387	1.46026	1.387016
	Affected	1.401	1.47500	1.401017
Basal	Normal	1.360	1.43184	1.360015
	Affected	1.380	1.45289	1.380016

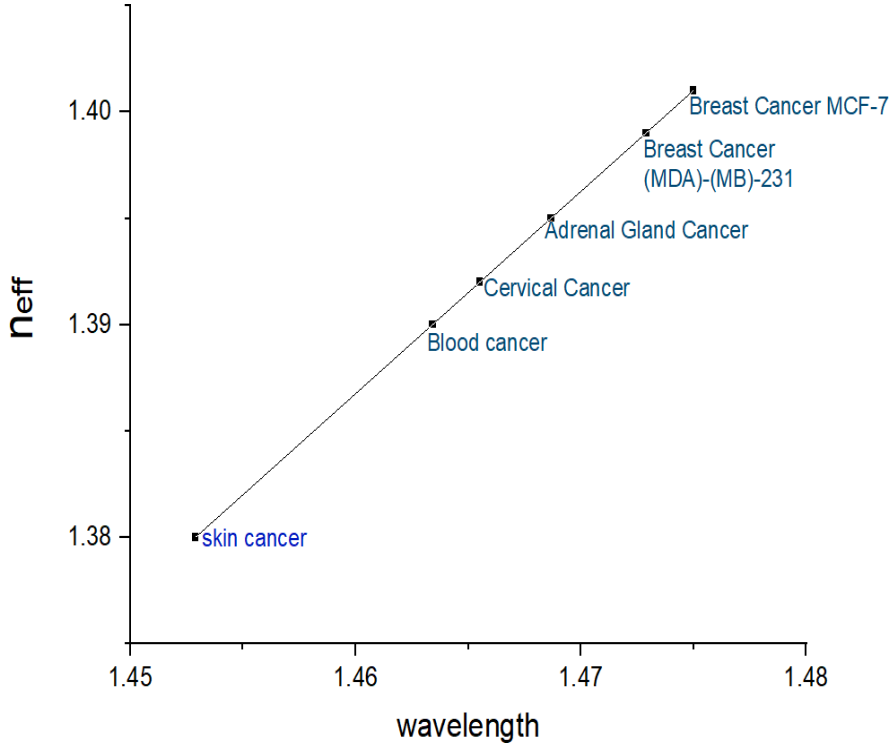

Figure 13. Effect of Wavelength on Relative Power of Fbg for Different Cancerous Cell

A shift in the Bragg wavelength results from this variation in the effective refractive index, which can be detected and correlated with the concentration of cancer biomarkers.

The dependence of resonant wavelength on the Grating of FBG was observed and analyzed for different cancerous cell, A FBG with a variable refractive index has its wavelength shift values calculated and plotted in Figure 12 & Figure 13. It can be observed that the wavelength shift has a linear relationship with the effective refractive index as it increases from the value of skin cancer to the value of Breast cancer.

6. Conclusion

Using the principle of Fiber Bragg Grating, a wavelength shift can be achieved with the refractive index of a normal cell and a cancer cell by a proper design. The modeling, simulation, features, and characteristics of FBG were introduced. The reflected wavelength, Full width at half maximum, and effective refractive index were analyzed considering the variation in the refractive index of the cancerous cell. It is observed that when the effective refractive index of the suggested FBG for cancer detection increases, the resonant wavelength shift also increases. These results provide insight into the relationship between FBG characterizations and offer a potential approach to the development of high-performance optical biosensors based on FBG, specifically for the detection of cancerous cells.

References

[1] S.C. Sharan, H.K. Dhruva, T.M. Anitha, N. Roy, P. Sharan, R.M. Moudgalya, (2024) FBG Sensor Design and Analysis for Early Detection of Cancer, In 2024 11th International Conference on Computing for Sustainable

Global Development (INDIACom), IEEE, India. [DOI]

[2] M. Al Ahmad, A. Najar, A. El Moutaouakil, N. Nasir, M. Hussein, S. Raji, A. Hilal-Alnaqbi, Label-free cancer cells detection using optical sensors. IEEE Access, 6, (2018) 55807-55814. [DOI]

[3] M.A. Riza, Y.I. Go, S.W. Harun, R.R. Maier, FBG sensors for environmental and biochemical applications—A review, IEEE sensors journal, 20(14), (2020) 7614-7627. [DOI]

[4] Prasad, S. Pant, S. Srivatzen, S. Asokan, A non-invasive breast cancer detection system using FBG thermal sensor array: A feasibility study, IEEE Sensors Journal, 21(21), (2021) 24106-24113. [DOI]

[5] T. Parvin, K. Ahmed, A.M. Alatwi, A.N.Z. Rashed, Differential optical absorption spectroscopy-based refractive index sensor for cancer cell detection. Optical Review, 28, (2021) 134-143.

[6] M.M. Werneck, R.C.S.B. Allil, B.A. Ribeiro, F.V. de Nazaré, A guide to fiber Bragg grating sensors. Current trends in short-and long-period fiber gratings, (2013) 1-24.

[7] F. Chiavaioli, F. Baldini, S. Tombelli, C. Trono, A. Giannetti, Biosensing with optical fiber gratings. Nanophotonics, 6(4), (2017) 663-679.

[8] H. Fukano, D. Watanabe, S. Taue, Sensitivity characteristics of multimode-interference optical-fiber temperature-sensor with solid cladding material, IEEE Sensors Journal, 16(24), (2016) 8921-8927. [DOI]

[9] A. Othonos, K. Kalli, G.E. Kohnke, Fiber Bragg gratings: fundamentals and applications in telecommunications and sensing, Boston: Artech house, 3(2), (1999).

[10] G.B. Hocker, Fiber-optic sensing of pressure and temperature, applied optics, 18(9), (1979)1445-1448. [DOI]

[11] W.P. Huang, Coupled-mode theory for optical waveguides: an overview, Journal of the Optical Society of America A, 11, (1994) 963-983. [DOI]

[12] T. Erdogan, Fiber grating spectra. Journal of lightwave technology, 15(8), (1997) 1277-1294. [DOI]

[13] S. Udoh, J. Njuguma, R. Prabhu, Modelling and simulation of fiber Bragg grating characterization for oil and gas sensing applications, In First International Conference on Systems Informatics, Modelling and Simulation, (2014) 213-218.

[14] M.A. Jabin, K. Ahmed, M.J. Rana, B.K. Paul, M. Islam, D. Vigneswaran, M.S. Uddin, Surface plasmon resonance based titanium coated biosensor for cancer cell detection, IEEE Photonics Journal, 11(4), (2019) 1-10. [DOI]

[15] X.J. Liang, A.Q. Liu, C.S. Lim, T.C. Ayi, P.H. Yap, Determining refractive index of single living cell using an integrated microchip. Sensors and Actuators A: Physical, 133(2), (2007) 349-354. [DOI]

[16] N.A. Elmahdy, M.F.O. Hameed, S.S.A. Obayya, B.M. Younis, Highly sensitive plasmonic-grating PCF biosensor for cancer cell detection. Optical and Quantum Electronics, 56(4), (2024) 688.

[17] D. Anastasopoulos, P. Moretti, T. Geernaert, B. De Pauw, U. Nawrot, G. De Roeck, F. Berghmans, E. Reynders, Identification of modal strains using sub-microstrain FBG data and a novel wavelength-shift detection algorithm. Mechanical Systems and Signal Processing, 86, (2017) 58-74. [DOI]

[18] M. Elsherif, A.E. Salih, M.G. Munoz, F. Alam, B. AlQattan, D.S. Antonysamy, M.F. Zaki, A.K. Yetisen, S. Park, T.D. Wilkinson, H. Butt, Optical fiber sensors: Working principle, applications, and limitations. Advanced Photonics Research, 3(11), (2022) 2100371. [DOI]

Acknowledgement

With great appreciation, I would like to thank Dr. Srinivasan N., Thiagarajar College's Dean of Research, for all of his help and assistance during this study effort. This research would not have been possible without the resources and research facilities provided by Dr. Preeta Sharan, Dean of Research at The Oxford College of Engineering, for which I am also deeply grateful. The Oxford College of Engineering, Bangalore's preetasharanlab provided support for this effort.

Funding

No funding was received for the conduct of this research

Conflict of interest

The authors declare that no conflict of interest exists.

Does the Article Screened for Similarity?

Yes.